Bioresource Technology 435 (2025) 132912

Contents lists available at ScienceDirect

Bioresource Technology

journal homepage: www.elsevier.com/locate/biortech

Elucidation of new sulfamethoxazole catabolic pathways in whole-cell catalyst of bacterium *Kocuria rhizophila* SA117

Tomáš Řezanka [a], Jiří Zahradník [b], Sofía G. Zavala-Meneses [a], Helena Marešová [a], Michal Řezanka [c], Helena Pelantová [a], Michal Grulich [a], Václav Filištein [d], Andrea Palyzová [a,*]

[a] Institute of Microbiology of the Czech Academy of Sciences, Vídeňská 1083, 142 00 Prague, Czech Republic
[b] First Faculty of Medicine, Charles University, BIOCEV, Průmyslová 595, 252 50 Vestec, Czech Republic
[c] Institute for Nanomaterials, Advanced Technologies and Innovation, Technical University of Liberec, Studentská 1402/2, 461 17 Liberec 1, Czech Republic
[d] Envisan-Gem, a.s., Geology, Ecology and Microbiology, Hůry 149, 373 71 Rudolfov, České Budějovice, Czech Republic

HIGHLIGHTS

- Genome annotation and proteomic analysis revealed catabolism of SMX.
- Whole-cell catalytic bioremediation of SMX by *Kocuria rhizophila* SA117.
- Thirty metabolites of $^{13}C_6$ and $^{2}H_3$-labeled SMX were identified as metabolic intermediates.
- Non-toxic metabolites of the Krebs cycle are formed by the degradation of SMX.

GRAPHICAL ABSTRACT

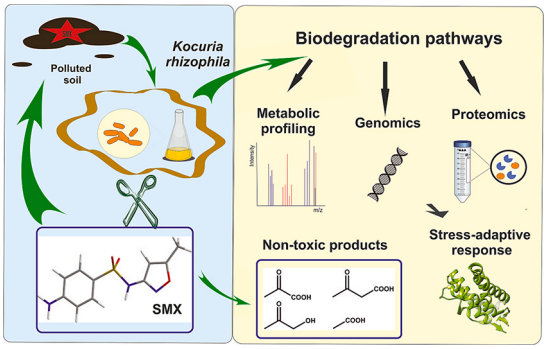

ARTICLE INFO

Keywords:
Biodegradation
Sulfonamide
Proteomics
Metabolic profiling
Genome sequencing

ABSTRACT

Sulfamethoxazole (SMX) and its residues exhibit high environmental persistence due to their resistance to conventional degradation processes. The bacterial strain *Kocuria rhizophila* SA117, isolated from polluted soils, was characterized biochemically, phylogenetically, and −omically. Herein, we describe a complete degradation pathway for SMX and determine two putative pathways: cleavage of the benzene ring and the degradation of the substituted isoxazole, leading to the formation of non-toxic Krebs cycle metabolites. Based on molecular structures containing $^{13}C_6$-labeled carbons and $^{2}H_3$ atoms, thirty metabolites were identified by high-resolution tandem mass spectrometry. Genomic and proteomic analysis of strain SA117 revealed its ability to perform a wide range of metabolic activities under sulfamethoxazole selective pressure. These activities include energy and sulfur metabolism, adaptation to stress conditions, and catabolism of aromatic compounds. This study has greatly

* Corresponding author.
E-mail addresses: rezanka@biomed.cas.cz (T. Řezanka), jiri.zahradnik@lf1.cuni.cz (J. Zahradník), szavala.meneses@biomed.cas.cz (S.G. Zavala-Meneses), maresova@biomed.cas.cz (H. Marešová), michal.rezanka@tul.cz (M. Řezanka), pelantova@biomed.cas.cz (H. Pelantová), grulich@biomed.cas.cz (M. Grulich), filistein@envisan.cz (V. Filištein), palyzova@biomed.cas.cz (A. Palyzová).

https://doi.org/10.1016/j.biortech.2025.132912
Received 5 March 2025; Received in revised form 26 June 2025; Accepted 26 June 2025
Available online 27 June 2025

enhanced the understanding of microbial sulfonamide degradation and highlighted the potential of the bacterium *Kocuria* in remediation strategies.

1. Introduction

Antibiotics are extensively used to treat diverse infectious diseases affecting humans and animals. This widespread use contributes to their pervasive presence in the environment, posing potential risks to human health. The introduction of antibiotics into the environment primarily occurs mainly through human and animal excreta, leading to their accumulation in wastewater (Karthikeyan & Meyer, 2006; Gibs et al., 2013; Wang & Wang, 2018). The effectiveness of conventional processes in wastewater treatment plants (WWTPs) in removing antibiotics is limited, resulting in their prolonged release and accumulation in the environment (Falås et al., 2016). Moreover, this persistence creates selective pressure on native organisms and may increase antibiotic-resistant bacteria and the spread of antimicrobial resistance genes (Rauseo et al., 2021).

Sulfonamides are an important class of synthetic antimicrobials with broad applications, such as antimicrobial, antidiabetic, diuretic, anticonvulsant, and herbicidal agents. Sulfamethoxazole (SMX), recognized as one of the most widely prescribed sulfonamides, effectively eradicates pathogens and treats infections caused by the *Enterobacteriaceae* family (Shah et al., 2013). The extensive consumption, chemical recalcitrance, and long half-life contribute to its persistence and frequent detection in various wastewaters, specifically in the ng/L-μg/L range in municipal WWTPs and reaching concentrations up to mg/L in hospital wastewater (Tian et al., 2019).

Several remediation technologies, including adsorption, ozonation, photolysis, and chemical or electrochemical oxidation, have been used for SMX removal (Wang et al., 2016; Hong et al., 2020). However, these technical strategies generate toxic byproducts, and elevated costs and economic inefficiencies associated with these methods may impede their integration into routine WWTP processes. Compared with these treatment technologies, microbial biodegradation emerges as a more environmentally friendly and cost-effective alternative, demonstrating versatility in application. Up to date some bacterial strains have been proved to be able to degrade SMX efficiently, like *Sphingobacterium mizutaii* LLE5 (Song et al., 2021), *Achromobacter denitrificans* PR1, *Microbacterium* sp. strain BR1, *Pseudomonas chrysosporium*, *P. stutzeri, Acinetobacter* sp. (Nguyen et al., 2018; Wang & Wang, 2018), *Rhodococcus equi* (Larcher and Yargeau, 2011), *Bacillus cereus* (Dong et al., 2022) and *P. silesiensis* (Liu et al., 2022).

Limited information is available on the structure of the non-toxic biodegradation products of SMX, as most reports focus only on microorganisms that reduce the contaminant of the parent compound. Three putative SMX degrading pathways have been reported so far: (1) the hydrolysis of sulfonamide S—N bond; (2) the N—O bond of isoxazole ring breaking and subsequent degradation; (3) deamination, hydroxylation, acetylation, and nitration (Herzog et al., 2013; Jia et al., 2017, Wang & Wang, 2018). Similarly, the various intermediates formed during the SMX biodegradation have been described. The structure of these metabolites can be divided into two main groups. The first group includes SMX modifications such as hydroxylation of the benzene ring or isoxazole (Mulla et al., 2018; Hou et al., 2022), reactions of the aromatic amino group (Nunes et al., 2020; Liu et al., 2022) or replacement of the amino group by glucuronic acid (Wang et al., 2021). The second group consists of low molecular weight metabolites formed during the biodegradation of SMX. However, all these metabolites are only partial intermediates, such as 1-aminophenol, benzene-triol, hydroquinone, or aminomethylisoxazole. Complete biodegradation by a single bacterial strain, except for metabolites formed during the early stages of the degradation process, has not yet been described.

Although SMX biodegradation has been extensively studied, many crucial aspects are still missing. This study describes the multi-omics background of the putative SMX degradation pathways by the fully characterized bacterium *Kocuria rhizophila* SA117, which has not yet been described as a potential degrader. The degradation pathways were designed based on metabolites identified by high-resolution tandem mass spectrometry (HR-MS/MS) and pyrolysis gas chromatography mass spectrometry (Py-GC–MS) using commercially available carbon-labeled ($^{13}C_6$-SMX) and deuterium-labeled ($^{2}H_3$-SMX) molecules (synthesized in the laboratory). Moreover, our findings were supported by the identification of several genes and proteins involved in the catabolism of aromatic compounds; thus, they are potentially involved in the degradation of SMX. Our results provide a very detailed insight into the issue of microbial metabolism under drug-induced stress conditions and thus support the ability to apply this degrader in bioremediation strategies, especially of sulfonamides, in various ecosystems.

2. Materials and methods

2.1. Chemicals

Standards of the molecules 4-amino-*N*-(5-methyl-3-isoxazolyl)benzenesulfonamide (SMX) and 4-amino-*N*-(5-methyl-3-isoxazolyl)benzene-$^{13}C_6$-sulfonamide ($^{13}C_6$-SMX) were purchased from Molekula Group (München, Germany) and Sigma-Aldrich (St. Louis, MO, USA), respectively. A sample of 3,5,4́-[$^{2}H_3$]-sulfamethoxazole ($^{2}H_3$-SMX or D_3-SMX) was prepared according to a previously reported procedure (Heinkele & Mürdter, 2007). Briefly, SMX (1.198 g) was dissolved in D_2O and D_2SO_4 and refluxed for 3 days. The reaction mixture was then extracted with ethyl acetate, dried, and recrystallized from ethanol. The procedure yielded 349 mg (29 %) of the title compound. High-resolution mass spectrometry (ESI^+): calculated for $C_{10}H_9D_3N_3O_3S$ $[M + H]^+$, 257.0782; found, 257.0769. The structure was verified by nuclear magnetic resonance (NMR). ^1H and ^{13}C NMR data were consistent with the previously published ones (Heinkele & Mürdter, 2007) (see Supplementary Material).

The solvent dimethyl sulfoxide (DMSO) required for stock solutions of SMX compounds was obtained from Penta Chemicals s.r.o. (Prague, Czech Republic). Other chemicals and reagents used in the analysis were of high analytical grade and obtained from Sigma-Aldrich. Media components were purchased from HiMedia Laboratory (Maharashtra, India).

2.2. Media and culture conditions

Luria-Bertani (LB) culture medium composed of 10 g/L tryptone, 5 g/L yeast extract, and 10 g/L NaCl was used for the pre-inoculum culture of the isolates. Selected isolates were screened for co-metabolic activity in minimal medium (M9) containing 0.5 g/L NaCl, 3.0 g/L K_2HPO_4, 14.62 g/L Na_2HPO_4, 1 g/L NH_4Cl supplemented with trace elements (M9TE; in mg/L: 200 $MgSO_4{\cdot}7H_2O$, 10 $CaCl_2{\cdot}2H_2O$, 6.6 $ZnSO_4{\cdot}7H_2O$, 0.17 $MnSO_4{\cdot}4H_2O$, 1.5 $FeSO_4{\cdot}7H_2O$, 0.48 $CoCl_2{\cdot}6H_2O$, 0.47 $CuSO_4{\cdot}5H_2O$, and 0.45 $Na_2MoO_4{\cdot}2H_2O$) and yeast extract (4 g/L; M9TEYE). SMX was added from stock solutions (5 mg in 0.5 mL of DMSO) to a 100 mg/L final concentration. To prepare solid media for screening and short-term maintenance, 22 g/L agar was added to LB and M9 media.

For the preparation of the whole-cell catalyst, biomass from precultures grown in LB medium (24 h at 28 °C) was harvested by centrifugation (10, 000 × g, 15 min, 10 °C), washed and resuspended in M9TE to a final concentration of 10 % (wet weight). The biodegradation study was performed as follows: 3 mL of the biomass was added into multiwell cell culture plates and supplemented with SMX, $^{13}C_6$-SMX, and $^{2}H_3$-

SMX. The reaction mixtures (in triplicate) were incubated on an orbital shaker (190 rpm) at 28 °C for 72 h. SMX, $^{13}C_6$-SMX, and $^{2}H_3$-SMX were added from stock solutions (5 mg in 0.5 mL of DMSO) to a 100 mg/L final concentration. For comparative proteomics experiments, 3 mL samples of the whole-cell catalyst were supplemented with glycerol (2 g/L), DMSO (1 *v/v*), or SMX (100 mg/L dissolved in DMSO) and cultivated (in triplicate) on an orbital shaker (190 rpm) at 28 °C for 72 h.

2.3. Isolation of SMX-tolerant strains

Soil samples were collected in the locality of Třeboň, Czech Republic, from a site contaminated with sewage sludge from a nearby WWTP (49.0322278N, 14.7556283E). Microorganisms were isolated using 5 g of soil subjected to a three-step enrichment in LB medium (28 °C, 24 h, 200 rpm). The resulting cultures were used for serial dilutions (10^1 – 10^6), and 0.1 mL of dilutions 10^4 and 10^6 were plated on solid M9 medium supplemented with SMX at a concentration of 100 mg/L. After 48 h of incubation at 28 °C, single colonies displaying distinct morphologies were transferred from agar plates to flasks containing 100 mL of M9TEYE liquid medium supplemented with SMX (100 mg/L) and cultured at 28 °C for 72 h. Cultures that emerged under the intensive selective pressure of SMX were subjected to morphological and biochemical characterization and screened for the potential degradation of SMX using spectrophotometric analysis (see Supplementary Material).

2.4. Phylogenetic identification and genome annotation

The isolate SA117 was grown overnight in LB media, and for genomic DNA extraction, the ZymoBIOMICS DNA Miniprep Kit (Zymo Research) was used following the manufacturer's instructions. Whole-genome sequencing and genome assembly was performed by an external facility (SEQme s.r.o, Dobříš, Czech Republic) using the Illumina NovaSeq platform. The genomic sequencing data was uploaded to the Type (Strain) Genome Server (TYGS, https://tygs.dsmz.de) for a whole genome-based taxonomic analysis. Pairwise sequence similarities were calculated by the TYGS server using Genome BLAST Distance Phylogeny (GBDP), and accurate inter-genomic distances were inferred under the algorithm "trimming" and distance formula d_5 (Meier-Kolthoff & Göker, 2019). The phylogenetic tree was constructed using the genomes of isolate SA117 and related taxa and inferred with FastME 2.1.6.1 from GBDP distances calculated from genome sequences. The digital DNA-DNA hybridization (dDDH) values between strain SA117 and the ten closest related strains were calculated using the Genome-to-Genome Distance Calculator (GGDC) v3.0 (https://ggdc.dsmz.de) (Meier-Kolthoffet al., 2022).

Additionally, average nucleotide identity (ANI) values between the isolate SA117 and 23 representative complete genomes of related species were estimated through pairwise genome alignment based on ANI-Blast (ANIb) and ANI-MUMmer (ANIm) algorithms available within the JspeciesWS web service (Richter et al., 2016).

The Rapid Annotation using Subsystem Technology server version 2.0 (RAST; https://rast.theseed.org, accessed on March 15, 2024) performed the functional annotation, gene calling, and gene mapping (Aziz et al., 2008). This Whole Genome Shotgun project has been deposited at DDBJ/ENA/GenBank under the accession JBNWVJ000000000. The BioProject ID in GenBank is PRJNA1263454.

2.5. Analysis of SMX metabolites by shotgun mass spectrometry

The whole-cell catalyst of *K. rhizophila* strain SA117 was cultured in M9TE medium supplemented with SMX, $^{13}C_6$-SMX, and 3,5,4'-[$^{2}H_3$]-SMX (final concentration of 100 mg/L). Intermediates of the SMX metabolic pathway were extracted from cell cultures as described by (Palyzová et al. 2019). Briefly, a 0.5 mL sample was extracted with 0.5 mL of *tert*-butyl methyl ether under vigorous shaking on a vortex mixer (10 min). The organic and water phases were separated by centrifugation (12,000 × *g* for 10 min). The organic phases were used for high-resolution electrospray ionization mass spectrometry (HRESI). An LTQ-Orbitrap Velos mass spectrometer (Thermo Fisher Scientific, San Jose, CA, USA) equipped with a heated electrospray interface was operated in positive and negative ionization modes. The mass spectrometry scan range was performed in the Fourier transform cell and recorded within a window between 50 and 300 Da. The mass resolution was set to 105,000, and the ion spray voltage was set at 3.5 kV (in positive ionization mode) and −2.5 kV (in negative ionization mode). Both ionization modes used the following parameters: sheath gas flow, 18 arbitrary units (AU); auxiliary gas flow, 7 AU; ion source temperature, 250 °C; capillary temperature, 230 °C; capillary voltage, 50 V; tube lens voltage, 170 V. Helium was used as a collision gas for collision-induced dissociation (CID) experiments. The CID normalization energy of 35 % was used to fragment parent ions. The MS spectrometer was calibrated using a Pierce LTQ Orbitrap positive and/or negative ion calibration solution (Thermo Fisher Scientific). The internal lock mass was used in mass spectra acquisition (i.e., 255.2330 Da $[M-H]^-$ palmitic acid in the negative ESI). The mass accuracy was better than 2 ppm. The chemical structure of the compounds was confirmed with the help of the spectral database Metlin https://metlin.scripps.edu/ (Guijas et al., 2018).

2.6. Pyrolysis-gas chromatography-mass spectrometry

The analysis of volatile metabolites was performed by pyrolysis–gas chromatography-mass spectrometry (see Supplementary Material). Briefly, lyophilized bacteria were subjected to pyrolysis, and volatile compounds were analyzed by GC–MS. The mass spectrometry data, including tandem ESI($^{+,-}$)MS and EI MS, have been deposited to the Zenodo repository (https://zenodo.org/records/15498979).

2.7. Comparative proteomics experiments with LC/MS Q-TOF and data processing

The whole-cell catalyst of *K. rhizophila* strain SA117 was cultured in M9TE medium supplemented with SMX, DMSO, and glycerol as a control. Samples were cleaned using SpeedBead Magnetic Carboxylate (Cytiva, Marlborough, MA, USA) beads and digested with trypsin overnight at 37 °C. The analysis was performed on a Vanquish liquid chromatography system (LC, Thermo Scientific, Waltham, MA, USA) connected to the timsToF SCP mass spectrometer equipped with CaptiveSpray (Bruker Daltonics, Bremen, Germany). The mass spectrometer was operated in a positive data-independent mode. One microliter of peptide mixture was injected by an autosampler onto the C18 trap column (Pepmap Neo C18 5 μm, 0.3x5 mm, Thermo Scientific). After trapping, the peptides were eluted from the trap column and separated on a C18 column (Pepsep C18 150x0.15 mm, 1.5 μm, Bruker Daltonics) using a 35 min linear water-acetonitrile gradient from 5 % (*v/v*) to 35 % (*v/v*) acetonitrile at a flow rate of 1.0 μL/min. The trap and analytical columns were both heated to 50 °C. The *m/z* range was between 100 and 1700. The number of PASEF was 5, and the total cycle time was 1.04 s. The target intensity was 14,000, and the intensity threshold was 500.

The raw data were processed using DIA-NN software Metlin Metabolite Searching Home Page, https://metlin.scripps.edu/ (accessed 2024-05-15) (Demichev et al., 2020) and analyzed by Perseus software (Tyanova et al., 2016) with a threshold *p*-value of 0.05. To establish a more comprehensive link between proteomic and genomic data, the RAST and Prokka software tools were employed (Seemann, 2014) with downstream translation by BioPython Seq module (Python 3.10.4). Identified hits were manually curated and searched against the related *Kocuria* reference strains.

The mass spectrometry proteomics data, including primary data, have been deposited to the Zenodo repository (https://zenodo.org/records/15498979).

3. Results and discussion

3.1. Isolation, screening, and identification of SMX-degrading bacteria

More than one hundred bacterial isolates were obtained from the polluted soil enrichment and examined for potential degradation under SMX selection pressure at a dose corresponding to 100 mg/L therapeutic drug concentration. During screening in a liquid medium using a co-metabolism strategy, six bacterial isolates were selected for growth tolerance to SMX and degradation potential. While most of these selected isolates displayed very low removal efficiency, only one isolate exhibited an effective reduction in SMX concentration of 83 % (see Supplementary Material**)**. The isolate was designated as the strain SA117, and its conventional morphological and biochemical characterization was performed by the German Collection of Microorganisms and Cell Cultures GmbH (DSMZ Braunschweig, Germany) (see Supplementary Material).

Whole–genome sequencing revealed the taxonomic classification and evolutionary relationships of the strain *K. rhizophila* SA117. Based on whole-genome sequencing, the relationship between strain SA117 and related type strains is shown by the phylogenetic tree (Fig. 1). The calculated digital DNA-DNA hybridization (dDDH) value between strain SA117 and *K. rhizophila* TA68 was 79 % with a GC content difference of 0.04 %. This dDDH value is higher than the standard expected cut off of 70–79 %, where organisms ranked below 70 % are considered as different species (Meier-Kolthoff et al., 2013). The strain SA117 was clustered with three species of the *Kocuria* genus: *K. rhizophila* (strain TA68), *K. tytonis* (strain DSM104130), and *K. tytonicola* (DSM104133T). 16S-based comparison showed a 99.76 % similarity to *K. rhizophila* TA68 and 98 % to *K. rhizophila* 4R-31 (see Supplementary Materials). The difference in GC content (in percentage) was 0.04 between strain SA117 and *K. rhizophila* TA68, 0.14 with *K. tytonis* DSM 104130, and 0.37 compared to *K. tytonicola* DSM 104133^{T}. Given the standard convention of ANIb values of equal to or higher than 95 % for strains to be regarded as members of the same genomic species (Arahal, 2014), the 97 % ANIb value confirms the affiliation of strain SA117 to the *K. rhizophila* species.

3.2. Genes associated with metabolic pathways

Based on the RAST annotation, 52 RNA genes were found, and 2,346 protein-encoding genes were predicted. These genes were grouped into 243 subsystems. Of these, amino acids and derivatives (206), protein metabolism (157), carbohydrates (156), vitamins, prosthetic groups, and pigments (118) were the most abundant categories. Throughout the genome of strain SA117, the key genes connected with SMX degradation pathways were revealed and represented approximately 15.3 % of the whole genome (Fig. 2). Three genes encoding amidohydrolase proteins were identified in different locations within the genome of strain SA117. One of them is a gene cluster encoding Rieske domain protein (2Fe-2S), sulfur acceptor protein SufE, thiosulfate sulfurtransferase, and rhodanese (EC 2.8.1.1). Initially identified in *P. putida* as key enzymes in the degradation of aromatic compounds, Rieske oxygenases are now recognized for their broader role in catalyzing diverse oxidative transformations across various catabolic and biosynthetic pathways, with promising applications in environmental remediation. These oxygenases are known to utilize substrates with a wide range of chemical structures, such as aromatics, pharmaceuticals, and hydrocarbons (Bopp et al., 2024). Next cluster included genes encoding acetolactate synthase and L-aspargine permease (EC 3.5.1.1), and the last identified amidohydrolase gene encodes for *N*-carbamoyl- L-amino acid amidohydrolase (EC 3.5.1.87). Likewise, the gene responsible for encoding dihydropteroate synthase (EC 2.5.1.15) was located. This enzyme catalyzes *para*-aminobenzoate condensation, indicating its likely role in efficient SMX biodegradation (Wu et al., 2023). Interestingly, eight genes encoding monooxygenases were found in the genome, two of which are antibiotic biosynthesis monooxygenases. The remaining monooxygenase genes are

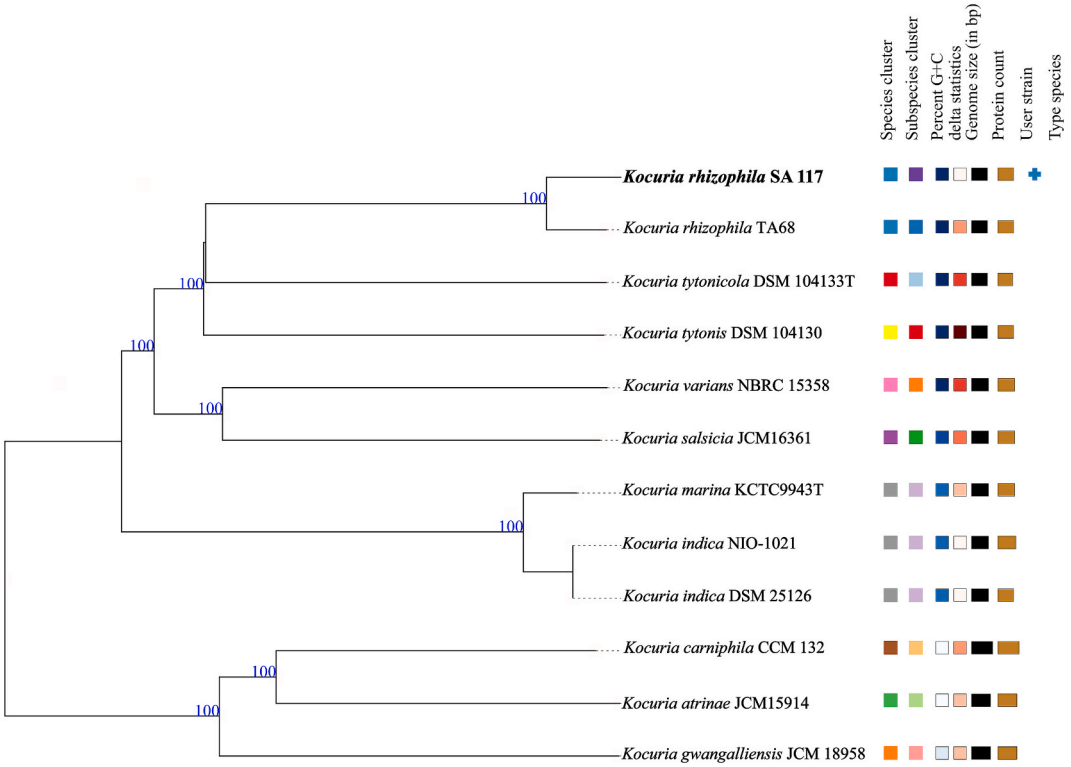

Fig. 1. Phylogenomic tree based on TYGS results showing the relationship between the draft genome of strain SA117 with related type strains. Values above branches are GBDP pseudo-bootstrap support values >60 % from 100 replications, with an average branch support of 88.9 %. The tree was rooted at the midpoint. *K. rhizophila* SA117 is depicted in bold. The same color indicates the same species cluster.

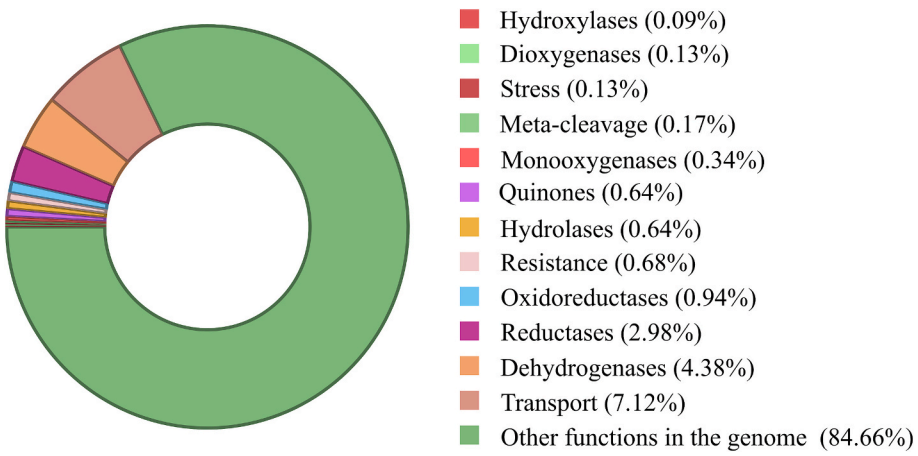

Fig. 2. Genomic overview of strain *K. rhizophila* SA117. The schematic representation shows the genes encoding functions primarily involved in the degradation of SMX in relation to the whole genome (as percentage).

nitrilotriacetate monooxygenase, flavin family monooxygenase, siderophore monooxygenase, and a luciferase-like monooxygenase. Notably, several genes encoding cytochrome *c* (cyt *c*) were found in the genome. In *Shewanella* species, cyt *c* grants respiratory versatility, which confers bacteria with a high potential to be used in bioremediation (Guo et al., 2022).

Concerning sulfur metabolism, several genes involved were found in SA117s genome. Noteworthy is the identification of the iron-sulfur gene cluster encoding SufB, C, D, R, and E, which was found and is known to be induced under oxidative stress conditions (Goldsmith-Fischman et al., 2004). A complete list of the identified genes with further details was deposited in the Zenodo repository under url: https://zenodo.org/records/15498979.

3.3. Biodegradation pathways of SMX: Metabolite and enzyme profiling

To elucidate the biodegradation mechanism of SMX in *K. rhizophila* SA117, an integrative approach combining proteomic analysis and high-resolution mass spectrometry was employed. This enabled the identification of key enzymes and intermediate metabolites involved in the biodegradation of SMX. According to the chemical structure and mass spectrum, analysis of cell extracts revealed the presence of 30 metabolites leading towards the proposed metabolic pathway for biodegradation of SMX, which were divided into two parts: biodegradation of the benzene ring (pathway I) and biodegradation of the substituted isoxazole (pathway II).

3.3.1. Biodegradation pathway I: Aromatic ring cleavage and downstream metabolism

Shotgun analysis was conducted using an LTQ Orbitrap Velos instrument with HRESI to detect and identify biodegradation products. To facilitate the complete degradation process of the SMX molecule, strain SA117 was incubated with $^{13}C_6$-SMX and $^{2}H_3$-SMX. Molecular ions exhibiting a high ^{13}C content were identified by MS/MS (see Supplementary Material).

Namely, eight compounds retained the structure of the benzene ring of the SMX molecule, five of which molecules had structures that indicated subsequent cleavage of double bonds between carbon atoms (see Supplementary Material). We detected four products as SMX building blocks, identified as 4-aminophenol (M1), benzene-1,2,4-triol (M2), hydroquinone (M3), and (*2Z,4E*)-4-hydroxy-6-oxohexa-2,4-dienoic acid (γ-hydroxymuconic semialdehyde) (M5) corresponding to previously published data (Mulla et al., 2018). Among the catalyst-associated enzymes, amidohydrolase, putative FAD-binding monooxygenase, and 3-hydroxybenzoate 4-monooxygenase were found in the studied proteome and likely initiated SMX degradation by the cleavage of the sulfonamide bond, generating initial building block 4-aminophenol (M1). Subsequently the metabolic transformation proceeds through hydroxylation steps facilitated by 3,4-dihydroxyphenylacetate 2,3-dioxygenase and α-ketoglutarate-dependent dioxygenase AlkB, generating benzene-1,2,4-triol (M2) and hydroquinone (M3) (Fig. 3). These are subsequently cleaved oxidatively to form ^{13}C-labeled molecules, namely (2*E*,4*Z*)-3-hydroxyhexa-2,4-dienedioic-1,2,3,4,5,6-$^{13}C_6$ acid (M4a) and (2*Z*,4*E*)-4-hydroxy-6-oxohexa-2,4-dienoic-1,2,3,4,5,6-$^{13}C_6$ acid (M5).

In addition to four deuterium-containing compounds, two additional intermediates (*2E,4Z*)-3-hydroxyhexa-2,4-dienedioic-5-D acid (M12a) and (*2E,4Z*)-3-hydroxyhexa-2,4-dienedioic-2,4-D_2 acid (M16a) represent the first detectable compounds undergoing benzene ring cleavage (Fig. 3, see Supplementary Material). We identified the molecule (*2Z,4E*)-4-hydroxy-6-oxohexa-2,4-dienoic-1,2,3,4,5,6-$^{13}C_6$ acid on the tandem mass spectrum, which suggests that the SMX degradation pathway I proceed in the same direction by the whole-cell catalyst of strain SA117. From the psedomolecular ion $[^{13}C_6H_5O_4]^-$, there is a loss of $^{13}CO_2$ in MS/MS to form an ion at *m/z* 102.0463 and another loss of H_2O to form an ion at *m/z* 84.0357 ($[^{13}C_5H_3O]^-$).

High-resolution tandem mass spectra confirm the structure of the next biodegradation products M6, M7, and M8 formed by biodegradation pathway I (Fig. 3). These derivatives, which contain an aromatic ring and other biodegradation products (compounds M4b, M6, and M7), have previously been described (Ottosen et al., 2024; Tian et al., 2024). By enol-keto tautomerism, the compound M5 changes to a "keto" form, and by oxidation of the aldehyde group, a diacid (M4b, M12b, M16b) is formed. The reduction of double bonds produces 3-oxoadipic acid. This β-keto acid (M6, M13, M17), as β-ketoadipyl-CoA, is cleaved by β-ketoadipyl CoA thiolase into two CoAs (i.e., acetyl-CoA and succinyl-CoA), where both acids were detected as free acids (Brinkrolf et al., 2006).

All the above-mentioned metabolites were identified based on the molecule structures containing carbons labeled with ^{13}C or ^{2}H atoms (see Supplementary Material). Based on the synthesized molecule of SMX containing three deuterium atoms in the molecule, two of which were substituted on the benzene ring, it was possible to confirm the biodegradation pathway obtained from $^{13}C_6$-SMX (Fig. 3). The structure of succinic and acetic acids (M7, M8, M14, and M15) was proven by HR-MS/MS (see Supplementary Material). Succinic acid, labeled both ^{2}H and ^{13}C, cleaves H_2O and CO_2 from the pseudomolecular ion at *m/z* 118.0251 (M14), and the respective *m/z* 121.0326 (M7) to form the ions $[C_4H_2DO_3]^-$, and $[C_3H_4DO_2]^-$, $[^{13}C_4H_3O_3]^-$, and $[^{13}C_3H_5O_2]^-$, respectively. Acetic-2D acid, the respective acetic-$^{13}C_2$ acid, also loses water from the ion at *m/z* 60.0196 (M15) (or at *m/z* 61.0205; M8) to form the ion 42.0090 (or at *m/z* 43.0099) (https://zenodo.org/records

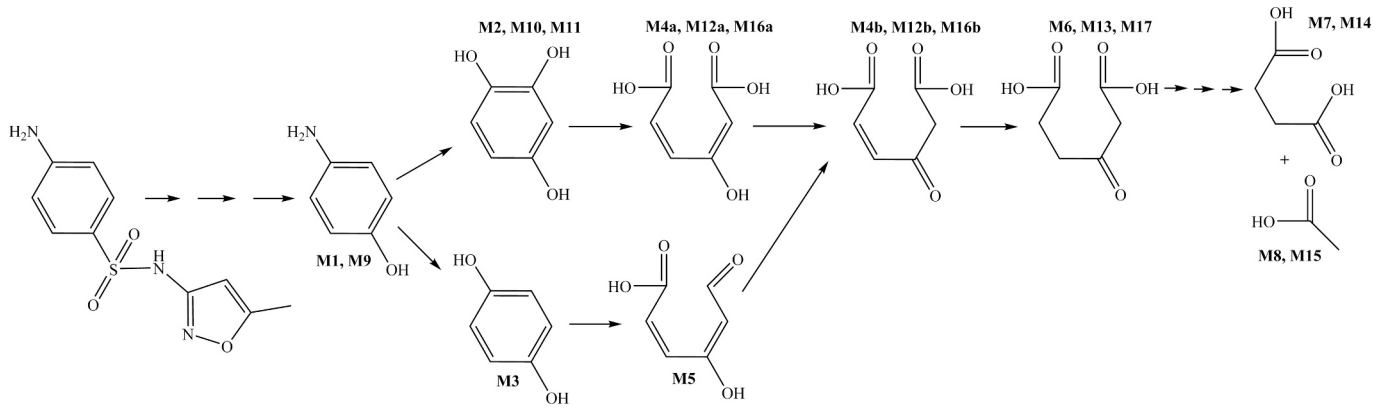

Fig. 3. Putative degradation pathway I of benzene ring via dioxygenase attack: 4-aminophenol, benzene-1,2,4-triol, hydroquinone, (*Z*)-4-oxohex-2-enedioic acid, 3-oxohexanedioic acid, succinic acid, and acetic acid. Most metabolites were confirmed by carbon-labeled stable isotope ($^{13}C_6$) and deuterium-labeled stable isotope ($^{2}H_3$). Given the identified products – 4-aminophenol, benzene-1,2,4-triol, and hydroquinone – the pathway likely involves *meta*-cleavage step with 1,2-dioxygenase. No known enzyme with 1,2-dioxygenase activity was identified in the genome and proteome, and therefore, other dioxygenase acting on substrates beyond their primary biological targets is involved, such as 3,4-dihydroxyphenylacetate 2,3-dioxygenase (detected in proteome) or alpha-ketoglutarate-dependent dioxygenase AlkB (detected in genome).

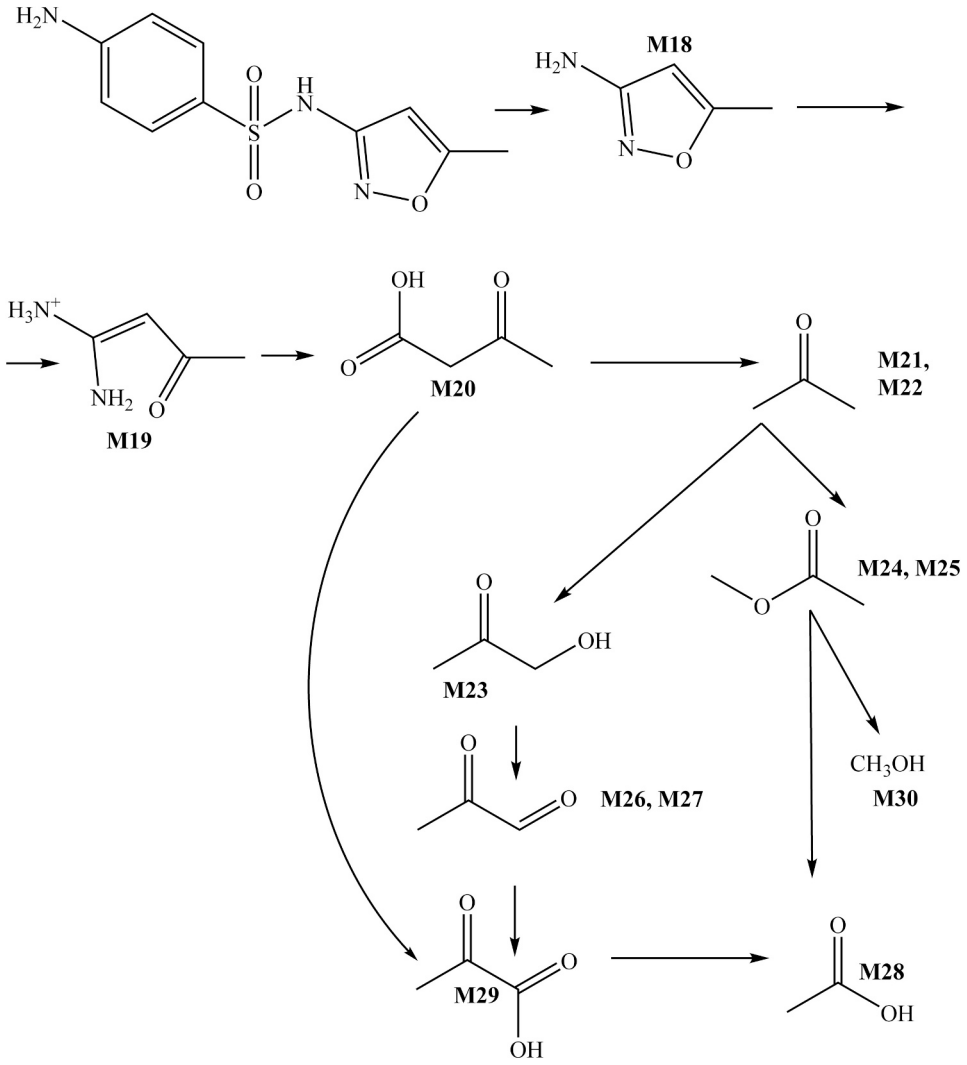

Fig. 4. Putative degradation pathway II of the substituted isoxazole created via amidohydrolase cleavage, opened by monooxygenase attack and ongoing from 5-methylisoxazol-3- amine to 3-oxobutanoic acid, acetone, and metabolites of the Krebs cycle. The metabolites were confirmed by deuterium labeled stable isotope ($^{2}H_3$) molecule of SMX.

/15498979). Our data revealed that both molecules of $^{13}C_6$-SMX and $^{2}H_3$-SMX were progressively biodegraded to two acids, i.e., succinic and acetic acids (Fig. 3). Both acids enter or participate in the Krebs cycle.

3.3.2. *Biodegradation pathway II: Substituted isoxazole degradation*

The second phase of SMX degradation, inferred from identified metabolites, involves multiple enzymatic steps, including ring opening, oxidation, reduction, and methylation. SMX degradation-associated proteins, deoxyribose-phosphate aldolase, nitrate reductase, and S-ribosylhomocysteine lyase, previously reported in *P. silesiensis* F6a (Liu et al., 2022), were also detected in the proteome of *K. rhizophila* SA117, suggesting their potential involvement in isoxazole ring opening. However, the difference in their abundance was not statistically significant.

The hypothetical biodegradation pathway II of a five-membered heterocycle specifically substituted isoxazole (5-methylisoxazol-4-D-3-amine, M18) is shown in Fig. 4. This compound, derived from the parent molecule of SMX, undergoes further metabolism through various primary intermediates via different biodegradation pathways (see Supplementary Material). The production of isoxazole (M18), which is formed by hydrolysis of the S—N bond, is confirmed by the overexpression of sulfurtransferase (a rhodanese-like domain-containing protein) involved in cyanide detoxification and/or peptide-methionine (*R*)-S-oxide reductase MsrB (Fig. 5**A**).

It is important to note that only metabolites containing one deuterium atom were identified. Many more biodegradation pathways exist, but if a metabolite is not labeled with a stable isotope, it cannot be distinguished from the unlabeled metabolites produced by the cell. It is obvious that the first biodegradation reaction took place by opening the isoxazole cycle to form compound ((*E*)-1-amino-3-oxobut-1-en-2-D-1-aminium, M19) (Fig. 4). Both 5-methylisoxazol-4-D-3-amine (M18) and M19 metabolites have been described in a study related to the effect of earthworm and gut bacteria activity on indigenous soil bacteria associated with SMX degradation (Zhang et al., 2022). In their review, Ottosen et al. (2024) state that the identification of compound M18 was described in six papers as a biodegradable product. Furthermore, this biodegradable product has also been identified in the paper (Plaisance et al., 2024). The significant difference in toxicity between compounds M18 and M19 must be emphasized at this point (Jin et al., 2024). The acute and chronic toxicity of compound M19, i.e., after the opening of the isoxazole ring, decreased dramatically in algae, daphnia, and fish. Other metabolites, particularly compounds M20 to M30 (see Supplementary Material), are expected to be either non-toxic or slightly toxic to cells. Dyrda et al. (2019) describe the toxicity of organic solvents, including methanol, in selected microorganisms, e.g., *Escherichia coli* and *Bacillus subtilis*. The viable count (%) in cultures treated with 4.8 % methanol was 63.2 for *B. subtilis* and 52.3 for *E. coli*. This methanol concentration is many orders of magnitude higher than the amount of methanol produced by the biodegradation of SMX. Metabolite conversion from M20 to M25 is catalyzed by acetoacetate decarboxylase (M20 to M21) and 3-ketoacyl-CoA (M21 to M24, M25). Both enzymes were detected in the proteome (https://zenodo.org/records/15498979). The two final metabolites (acetic acid M28 and methanol M30) can either be oxidized to water and carbon dioxide or further incorporated into the cell metabolites. Volatile metabolites specifically compounds M21 to M25 and M30, were identified by Py-GC–MS (https://zenodo.org/records/15498979). The use of a capillary column allowed the separation and identification of positional isomers, such as 1-hydroxypropan-2-one-1-D (M22) versus 1-hydroxypropan-2-one-3-D (M23) or methyl acetate-2-D (M24) versus methyl-D acetate (M25). For example, acetic-$^{13}C_2$ acid (M8) and acetic-2-D acid (M15) were identified as volatile metabolites using HR-MS/MS. The presence of isopropanol as a biodegradation product of SMX was also described using a microbial fuel cell (Wang et al., 2016).

3.4. *Proteomic response to SMX exposure*

The comparative proteomic analysis of *K. rhizophila* SA117 under SMX pressure revealed a stress-adaptive response and suggested the potential involvement of SMX-degrading enzymes. Incubation in a minimal medium supplemented with SMX, DMSO (solvent control), or glycerol (positive metabolic control) resulted in modest proteomic changes, with the most pronounced differences observed between the SMX- and glycerol-treated samples after 48 h. Using the annotated genome and identified proteins as a reference, 1,691 proteins present in more than one sample were detected. In contrast, the number of proteins showing statistically significant changes was relatively low, particularly at the 24-hour time point, where only 24 proteins were differentially expressed between the SMX and glycerol conditions. This number increased to 104 proteins after 48 h.

Glycerol, an efficient carbon and energy source, triggered a broader proteomic response indicative of enhanced metabolic activity. In contrast, SMX exposure led to the significant upregulation of proteins associated with cellular stress adaptation, including adenylate kinase, co-chaperonin GroES, peptidyl-prolyl *cis–trans* isomerase, peptidoglycan DD-metalloendopeptidase, lipase, and cold-shock proteins (Fig. 5**B**).

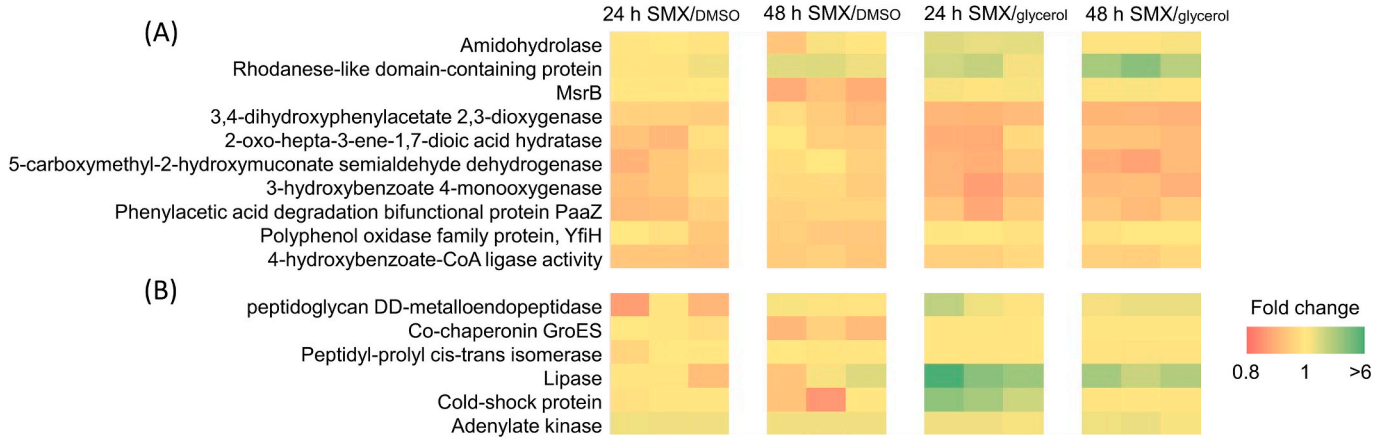

Fig. 5. Heat map of proteomics profiles of: (A) putative proteins involved in SMX degradation by the whole-cell catalyst SA117 and (B) significantly unrepresented stress response-associated proteins identified in the SA117 strain cells during whole-cell catalyst SMX degradation. Each row represents a distinct protein, while each column corresponds to a set of samples collected within a defined time range and conditions. The color scale coloring indicates changes in protein expression: red represents up-representation in the proteome, green indicates down-representation, and yellow highlights no change or limited change in protein abundance. (For interpretation of the references to color in this figure legend, the reader is referred to the web version of this article.)

Notably, adenylate kinase, a central enzyme in maintaining intracellular ATP levels, plays a crucial role in regulating bacterial growth under energetic stress (Thach et al., 2014), underscoring the cellular response to SMX-induced pressure.

Further proteomic profiling revealed the presence of proteins associated with the degradation of aromatic compounds, particularly those implicated in the 4-hydroxyphenylacetate catabolic pathway (Rodríguez-Castro et al., 2024). Although the different expression of these proteins did not reach statistical significance when compared to glycerol-supplemented samples (Fig. 5**A**), their detection supports a potential role in the transformation of SMX intermediates, such as 4-hydroxyaniline, which was also confirmed by metabolomic profiling. Importantly, control treatments using DMSO verified that the observed biochemical changes and degradation activities are attributable to SMX exposure rather than to solvent effects.

Genomic and proteomic data suggest that *K. rhizophila* SA117 utilizes a degradation pathway distinct from those characterized in other Actinobacteria. Specifically, the cluster of genes (*sad*A, *sad*B and *sad*C), encoding flavin-dependent monooxygenase and reductase involved in sulfonamide degradation in *Microbacterium* sp. BR1 and *Paenarthrobacter* sp. A01 (Ricken et al., 2017; Cao et al., 2019), was absent in the genome of SA117. Instead, the overall degradation profile and metabolic adaptation patterns of SA117 exhibited stronger similarity to those of *Pseudomonas* spp., indicating the involvement of alternative SMX transformation pathways.

4. Conclusion

Although sulfonamide antibiotics and their derivatives have been extensively studied, their subsequent biodegradation remains poorly understood. These metabolites frequently occur at higher concentrations, posing a greater risk. This study introduces *K. rhizophila* SA117, a strain with a significant biodegradation potential, and explores its complete genomic and biochemical profile, and its ability to metabolize SMX. Genomic, proteomic, and metabolic analyses revealed the complete SMX degradation through the cleavage of the benzene and isoxazole rings resulting in the production of non-toxic metabolites. A total of thirty ^{13}C and ^{2}H –labeled metabolites were identified by HR-MS/MS. Key enzymes involved in C—S bond and ring cleavage, S—N hydrolysis, and aromatic catabolism were confirmed. Additionally, stress-response proteins such as peptidoglycan DD-metalloendopeptidase, co-chaperonin GroES, and peptidyl-prolyl *cis–trans* isomerase upregulation suggested their role in adaptation to SMX exposure. These findings underscore the potential of *K. rhizophila* for the remediation of sulfonamide-contaminated environments.

CRediT authorship contribution statement

Tomáš Řezanka: Writing – original draft, Visualization, Methodology. **Jiří Zahradník:** Writing – review & editing, Investigation, Funding acquisition, Data curation. **Sofía G. Zavala-Meneses:** Writing – review & editing, Visualization, Methodology, Formal analysis. **Helena Marešová:** Methodology, Investigation, Formal analysis. **Michal Řezanka:** Writing – review & editing, Methodology, Investigation. **Helena Pelantová:** Methodology, Formal analysis, Data curation. **Michal Grulich:** Writing – review & editing, Visualization, Data curation. **Václav Filištein:** Resources, Methodology, Investigation. **Andrea Palyzová:** Writing – review & editing, Supervision, Project administration, Funding acquisition, Conceptualization.

Declaration of competing interest

The authors declare that they have no known competing financial interests or personal relationships that could have appeared to influence the work reported in this paper.

Acknowledgements

This research was funded by the Institutional Research Concept RVO 61388971 (Institute of Microbiology, Prague, Czech Republic), the Ministry of Education, Youth and Sports of the Czech Republic grant Microorganisms in Ecological Remediation – Bacteria as Cell Factories for Controlled Bioremediation of Ecosystems (CZ.02.01.01/00/23_020/0008502, to Andrea Palyzová) and grant Talking Microbes – Understanding Microbial Interactions within One Health Framework (CZ.02.01.01/00/22_008/0004597, to Andrea Palyzová), the project of National Institute of Virology and Bacteriology, Programme EXCELES, funded by the European Union, Next Generation EU (LX22NPO5103, to Jiří Zahradnik). We acknowledge CF MS of CIISB, Instruct-CZ Centre, supported by MEYS CR (LM2023042) and European Regional Development Fund-Project „Innovation of Czech Infrastructure for Integrative Structural Biology “(No. CZ.02.01.01/00/23_015/0008175).

Appendix A. Supplementary data

Supplementary data to this article can be found online at https://doi.org/10.1016/j.biortech.2025.132912.

Data availability

Data will be made available on request.

References

Arahal, D.R., 2014. Chapter 6 - Whole-Genome analyses: Average nucleotide identity. In: Goodfellow, M., Sutcliffe, I., Chun, J. (Eds.), Methods in Microbiology, Vol. 41. Academic Press, pp. 103–122. https://doi.org/10.1016/bs.mim.2014.07.002.

Aziz, R.K., Bartels, D., Best, A.A., DeJongh, M., Disz, T., Edwards, R.A., Formsma, K., Gerdes, S., Glass, E.M., Kubal, M., Meyer, F., Olsen, G.J., Olson, R., Osterman, A.L., Overbeek, R.A., McNeil, L.K., Paarmann, D., Paczian, T., Parrello, B., Pusch, G.D., Reich, C., Stevens, R., Vassieva, O., Vonstein, V., Wilke, A., Zagnitko, O., 2008. The RAST server: rapid annotations using subsystems technology. BMC Genomics 9 (1), 75. https://doi.org/10.1186/1471-2164-9-75.

Bopp, C.E., Bernet, N.M., Meyer, F., Khan, R., Robinson, S.L., Kohler, H.E., Buller, R., Hofstetter, T.B., 2024. Elucidating the role of O(2) uncoupling for the adaptation of bacterial biodegradation reactions catalyzed by Rieske oxygenases. ACS Environ. Au 4 (4), 204–218. https://doi.org/10.1021/acsenvironau.4c00016.

Brinkrolf, K., Brune, I., Tauch, A., 2006. Transcriptional regulation of catabolic pathways for aromatic compounds in *Corynebacterium glutamicum*. Genet. Mol. Res. 5 (4), 773–789. PMID: 17183485.

Cao, L., Zhang, J., Zhao, R., Deng, Y., Liu, J., Fu, W., Lei, Y., Zhang, T., Li, X., Li, B., 2019. Genomic characterization, kinetics, and pathways of sulfamethazine biodegradation by *Paenarthrobacter* sp. A01. Environ. Int. 131, 104961. https://doi.org/10.1016/j.envint.2019.104961.

Demichev, V., Messner, C.B., Vernardis, S.I., Lilley, K.S., Ralser, M., 2020. DIA-NN: neural networks and interference correction enable deep proteome coverage in high throughput. Nat. Methods 17 (1), 41–44. https://doi.org/10.1038/s41592-019-0638-x.

Dong, Z.K., Yan, X.J., Wang, J.H., Zhu, L.S., Wang, J., Li, C.Y., Zhang, W.J., Wen, S.F., Kim, Y.M., 2022. Mechanism for biodegradation of sulfamethazine by Bacillus Cereus H38. Sci. Total Environ. 809. https://doi.org/10.1016/j.scitotenv.2021.152237.

Dyrda, G., Boniewska-Bernacka, E., Man, D., Barchiewicz, K., Słota, R., 2019. The effect of organic solvents on selected microorganisms and model liposome membrane. Mol. Biol. Rep. 46 (3), 3225–3232. https://doi.org/10.1007/s11033-019-04782-y.

Falås, P., Wick, A., Castronovo, S., Habermacher, J., Ternes, T.A., Joss, A., 2016. Tracing the limits of organic micropollutant removal in biological wastewater treatment. Water Res. 95, 240–249. https://doi.org/10.1016/j.watres.2016.03.009.

Gibs, J., Heckathorn, H.A., Meyer, M.T., Klapinski, F.R., Alebus, M., Lippincott, R.L., 2013. Occurrence and partitioning of antibiotic compounds found in the water column and bottom sediments from a stream receiving two wastewater treatment plant effluents in Northern New Jersey, 2008. Sci. Total Environ. 458–460, 107–116. https://doi.org/10.1016/j.scitotenv.2013.03.076.

Goldsmith-Fischman, S., Kuzin, A., Edstrom, W.C., Benach, J., Shastry, R., Xiao, R., Acton, T.B., Honig, B., Montelione, G.T., Hunt, J.F., 2004. The SufE sulfur-acceptor protein contains a conserved core structure that mediates interdomain interactions in a variety of redox protein complexes. J. Mol. Biol. 344 (2), 549–565. https://doi.org/10.1016/j.jmb.2004.08.074.

Guijas, C., Montenegro-Burke, J.R., Domingo-Almenara, X., Palermo, A., Warth, B., Hermann, G., Koellensperger, G., Huan, T., Uritboonthai, W., Aisporna, A.E., Wolan, D.W., Spilker, M.E., Benton, H.P., Siuzdak, G., 2018. METLIN: a technology platform for identifying knowns and unknowns. Anal. Chem. 90 (5), 3156–3164. https://doi.org/10.1021/acs.analchem.7b04424.

Guo, K., Feng, X., Sun, W., Han, S., Wu, S., Gao, H., 2022. NapB restores cytochrome c biosynthesis in bacterial dsbD-deficient mutants. Commun. Biol. 5 (1), 87. https://doi.org/10.1038/s42003-022-03034-3.

Heinkele, G., Mürdter, T.E., 2007. Synthesis of [$^2H_3$]-labelled sulfamethoxazole and its main urinary metabolites. J. Label. Compd. Radiopharm. 50 (7), 656–659. https://doi.org/10.1002/jlcr.1375.

Herzog, B., Lemmer, H., Horn, H., Müller, E., 2013. Characterization of pure cultures isolated from sulfamethoxazole-acclimated activated sludge with respect to taxonomic identification and sulfamethoxazole biodegradation potential. BMC Microbiol. 13, 276–286. https://doi.org/10.1186/1471-2180-13-276.

Hong, M., Wang, Y., Lu, G., 2020. UV-Fenton degradation of diclofenac, sulpiride, sulfamethoxazole and sulfisomidine: degradation mechanisms, transformation products, toxicity evolution and effect of real water matrix. Chemosphere 258, 127351. https://doi.org/10.1016/j.chemosphere.2020.127351.

Hou, H., Mengting, Z., Duan, L., Zhao, Y., Zhang, Z., Yao, M., Zhou, B., Zhang, H., Hermanowicz, S.W., 2022. Removal performance and biodegradation mechanism of sulfonamides antibiotic contained wastewater by IFAS-MBR bioreactor. J. Mol. Liq. 367, 120572. https://doi.org/10.1016/j.molliq.2022.120572.

Jia, Y., Khanal, S., Zhang, H., Chen, G., Lu, H., 2017. Sulfamethoxazole degradation in anaerobic sulfate-reducing bacteria sludge system. Water Res. 119, 12–20. https://doi.org/10.1016/j.watres.2017.04.040.

Jin, Y., Yu, J., Yu, J., Wu, Y., Deng, S., Jiang, Y., Huang, Z., Wu, D., Zhu, W., 2024. Ce/N @BC prepared based on plant metallurgy strategy: a novel activator of peroxymonosulfate for the degradation of sulfamethoxazole. Environ. Pollut. 345, 123558. https://doi.org/10.1016/j.envpol.2024.123558.

Karthikeyan, K.G., Meyer, M.T., 2006. Occurrence of antibiotics in wastewater treatment facilities in Wisconsin, USA. Sci. Total Environ. 361 (1), 196–207. https://doi.org/10.1016/j.scitotenv.2005.06.030.

Larcher, S., Yargeau, V., 2011. Biodegradation of sulfamethoxazole by individual and mixed bacteria. Appl. Microbiol. Biotechnol. 91 (1), 211–218. https://doi.org/10.1007/s00253-011-3257-8.

Liu, X., Chen, J., Liu, Y., Wan, Z., Guo, X., Lu, S., Qiu, D., 2022. Sulfamethoxazole degradation by *Pseudomonas silesiensis* F6a isolated from bioelectrochemical technology-integrated constructed wetlands. Ecotoxicol. Environ. Saf. 240, 113698. https://doi.org/10.1016/j.ecoenv.2022.113698.

Meier-Kolthoff, J.P., Auch, A.F., Klenk, H.-P., Göker, M., 2013. Genome sequence-based species delimitation with confidence intervals and improved distance functions. BMC Bioinf. 14 (1), 60. https://doi.org/10.1186/1471-2105-14-60.

Meier-Kolthoff, J.P., Göker, M., 2019. TYGS is an automated high-throughput platform for state-of-the-art genome-based taxonomy. Nat. Commun. 10 (1), 2182. https://doi.org/10.1038/s41467-019-10210-3.

Meier-Kolthoff, J.P., Carbasse, J.S., Peinado-Olarte, R.L., Göker, M., 2022. TYGS and LPSN: a database tandem for fast and reliable genome-based classification and nomenclature of prokaryotes. Nucleic Acids Res. 50, D801–D807. https://doi.org/10.1093/nar/gkab902.

Mulla, S.I., Hu, A., Sun, Q., Li, J., Suanon, F., Ashfaq, M., Yu, C.-P., 2018. Biodegradation of sulfamethoxazole in bacteria from three different origins. J. Environ. Manage. 206, 93–102. https://doi.org/10.1016/j.jenvman.2017.10.029.

Nguyen, P.Y., Carvalho, G., Polesel, F., Torresi, E., Rodrigues, A.M., Rodrigues, J.E., Cardoso, V.V., Benoliel, M.J., Plósz, B.G., Reis, M.A.M., Oehmen, A., 2018. Bioaugmentation of activated sludge with *Achromobacter denitrificans* PR1 for enhancing the biotransformation of sulfamethoxazole and its human conjugates in real wastewater: kinetic tests and modelling. J. Chem. Eng. 352, 79–89. https://doi.org/10.1016/j.cej.2018.07.011.

Nunes, O.C., Manaia, C.M., Kolvenbach, B.A., Corvini, P.F.X., 2020. Living with sulfonamides: a diverse range of mechanisms observed in bacteria. Appl. Microbiol. Biotechnol. 104 (24), 10389–10408. https://doi.org/10.1007/s00253-020-10982-5.

Palyzová, A., Zahradník, J., Marešová, H., Řezanka, T., 2019. Characterization of the catabolic pathway of diclofenac in *Raoultella* sp. KDF8. Int. Biodeter. Biodegr. 137, 88–94. https://doi.org/10.1016/j.ibiod.2018.11.013.

Ottosen, C.F., Bjerg, P.L., Kümmel, S., Richnow, H.H., Middeldorp, P., Draborg, H., Lemaire, G.G., Broholm, M.M., 2024. Natural attenuation of sulfonamides and metabolites in contaminated groundwater – Review, advantages and challenges of current documentation techniques. Water Res. 254, 121416. https://doi.org/10.1016/j.watres.2024.121416.

Plaisance, A., Wayment, D., Raje, H., Boopathy, R., 2024. Biodegradation of sulfamethoxazole by a bacterium isolated from the Hurricane overtop sediments. Bioresour. Technol. Rep. 27, 101926. https://doi.org/10.1016/j.biteb.2024.101926.

Rauseo, J., Barra Caracciolo, A., Spataro, F., Visca, A., Ademollo, N., Pescatore, T., Grenni, P., Patrolecco, L., 2021. Effects of Sulfamethoxazole on growth and antibiotic resistance of a natural microbial community. Water 13 (9), 1262. https://doi.org/10.3390/w13091262.

Richter, M., Rosselló-Móra, R., Oliver Glöckner, F., Peplies, J., 2016. JSpeciesWS: a web server for prokaryotic species circumscription based on pairwise genome comparison. Bioinformatics 32 (6), 929–931. https://doi.org/10.1093/bioinformatics/btv681.

Ricken, B., Kolvenbach, B.A., Bergesch, C., Benndorf, D., Kroll, K., Strnad, H., Vlček, Č., Adaixo, R., Hammes, F., Shahgaldian, P., Schäffer, A., Kohler, H.-P.-E., Corvini, P.F. X., 2017. FMNH2-dependent monooxygenases initiate catabolism of sulfonamides in *Microbacterium* sp. strain BR1 subsisting on sulfonamide antibiotics. Sci. Rep. 7 (1), 15783. https://doi.org/10.1038/s41598-017-16132-8.

Rodríguez-Castro, L., Durán, R.E., Méndez, V., Dorochesi, F., Zühlke, D., Riedel, K., Seeger, M., 2024. The long-chain flavodoxin FldX1 improves the biodegradation of 4-hydroxyphenylacetate and 3-hydroxyphenylacetate and counteracts the oxidative stress associated to aromatic catabolism in *Paraburkholderia xenovorans*. Biol. Res. 57 (1), 12. https://doi.org/10.1186/s40659-024-00491-4.

Seemann, T., 2014. Prokka: rapid prokaryotic genome annotation. Bioinformatics 30 (14), 2068–2069. https://doi.org/10.1093/bioinformatics/btu153.

Shah, S.S.A., Rivera, G., Ashfaq, M., 2013. Recent advances in medicinal chemistry of sulfonamides. Rational design as anti-tumoral, anti-bacterial and anti-Inflammatory agents. Mini-Rev. Med. Chem. 13 (1), 70–86. https://doi.org/10.2174/1389557511307010070.

Song, J., Hao, G., Liu, L., Zhang, H., Zhao, D., Li, X., Yang, Z., Xu, J., Ruan, Z., Mu, Y., 2021. Biodegradation and metabolic pathway of sulfamethoxazole by *Sphingobacterium mizutaii*. Sci. Rep. 11 (1), 23130. https://doi.org/10.1038/s41598-021-02404-x.

Thach, T.T., Luong, T.T., Lee, S., Rhee, D.-K., 2014. Adenylate kinase from *Streptococcus pneumoniae* is essential for growth through its catalytic activity. FEBS Open Bio 4 (1), 672–682. https://doi.org/10.1016/j.fob.2014.07.002.

Tian, S.-Q., Wang, L., Liu, Y.-L., Yang, T., Huang, Z.-S., Wang, X.-S., He, H.-Y., Jiang, J., Ma, J., 2019. Enhanced permanganate oxidation of sulfamethoxazole and removal of dissolved organics with biochar: formation of highly oxidative manganese intermediate species and in situ activation of biochar. Environ. Sci. Technol. 53 (9), 5282–5291. https://doi.org/10.1021/acs.est.9b00180.

Tian, S., You, L., Huang, X., Liu, C., Su, J.-Q., 2024. Efficient sulfamethoxazole biotransformation and detoxification by newly isolated strain *Hydrogenophaga* sp. SNF1 via a ring ortho-hydroxylation pathway. J. Hazard. Mater. 480, 136113. https://doi.org/10.1016/j.jhazmat.2024.136113.

Tyanova, S., Temu, T., Cox, J., 2016. The MaxQuant computational platform for mass spectrometry-based shotgun proteomics. Nat. Protoc. 11 (12), 2301–2319. https://doi.org/10.1038/nprot.2016.136.

Wang, J., Wang, S., 2018. Microbial degradation of sulfamethoxazole in the environment. Appl. Microbiol. Biotechnol. 102 (8), 3573–3582. https://doi.org/10.1007/s00253-018-8845-4.

Wang, L., Liu, Y., Ma, J., Zhao, F., 2016. Rapid degradation of sulphamethoxazole and the further transformation of 3-amino-5-methylisoxazole in a microbial fuel cell. Water Res. 88, 322–328. https://doi.org/10.1016/j.watres.2015.10.030.

Wang, S., Yuan, R., Chen, H., Wang, F., Zhou, B., 2021. Anaerobic biodegradation of four sulfanilamide antibiotics: Kinetics, pathways and microbiological studies. J. Hazard. Mater. 416, 125840. https://doi.org/10.1016/j.jhazmat.2021.125840.

Wu, T., Guo, S.-Z., Zhu, H.-Z., Yan, L., Liu, Z.-P., Li, D.-F., Jiang, C.-Y., Corvini, P.-F.-X., Shen, X.-H., Liu, S.-J., 2023. The sulfonamide-resistance dihydropteroate synthase gene is crucial for efficient biodegradation of sulfamethoxazole by *Paenarthrobacter* species. Appl. Microbiol. Biotechnol. 107 (18), 5813–5827. https://doi.org/10.1007/s00253-023-12679-x.

Zhang, Y., Song, K., Zhang, J., Xu, X., Ye, G., Cao, H., Chen, M., Cai, S., Cao, X., Zheng, X., Lv, W., 2022. Removal of sulfamethoxazole and antibiotic resistance genes in paddy soil by earthworms (*Pheretima guillelmi*): intestinal detoxification and stimulation of indigenous soil bacteria. Sci. Total Environ. 851, 158075. https://doi.org/10.1016/j.scitotenv.2022.158075.